J. Fluid Mech. (2004), *vol.* 505, *pp.* 163–178.
DOI: 10.1017/S0022112004008298 Printed in the United Kingdom

Thermal winds forced by inhomogeneous boundary conditions in rotating, stratified, hydromagnetic fluid

By JOHN R. LISTER

Institute of Theoretical Geophysics, Department of Applied Mathematics and Theoretical Physics, University of Cambridge, Wilberforce Road, Cambridge CB3 0WA, UK

(Received 9 May 2003 and in revised form 8 October 2003)

Lateral variations in the thermal boundary conditions at the horizontal boundary of an otherwise stably stratified fluid layer drive circulatory motion. For a rapidly rotating electrically conducting fluid, the introduction of a background vertical magnetic field reduces the dimensionless strength of the thermal wind from $O(1)$ to $O(E^{1/4})$ for prescribed temperature variation or to $O(E^{1/2})$ for prescribed heat-flux variation, where E is the Ekman number. This is a significant effect when considering the spatially variable cooling of the Earth's core by the mantle. A general discussion of linear hydromagnetic flows identifies a large number of lengthscales inherent in the differential system as functions of the Ekman, Elsasser and stratification numbers, and shows that other scalings arise from the boundary conditions.

1. Introduction

Cooling of the Earth's fluid outer core drives convective motions with velocities of order $0.3\,\mathrm{mm\,s^{-1}}$ that are responsible both for the observed historic variation in the Earth's magnetic field and for the long-term maintenance of this field against ohmic decay by dynamo action. Most, if not all, of the outer core is thought to be vigorously mixed by compositional convection arising from solidification of the pure iron inner core from a multicomponent outer-core melt. However, there have been a number of suggestions that there might be a stably stratified layer at the top of the outer core under the boundary with the silicate mantle (e.g. Artyushkov 1972; Whaler 1980; Fearn & Loper 1981; Braginsky 1984, 1993; Lloyd & Gubbins 1990; Lay & Young 1990), particularly if the rate of cooling by the overlying mantle is subadiabatic (Gubbins, Thomson & Whaler 1982; Labrosse, Poirier & Le Mouël 1997; Lister & Buffett 1998). Since the mantle convects much more sluggishly than the core (by a factor of order 10^9), it imposes a thermal heat-flux boundary condition on the core that is steady on the timescale of core motions but spatially varying around the core–mantle boundary. Various attempts have been made to link variations in mantle temperatures inferred from seismic tomography with core flows inferred from variation of the magnetic field (e.g. Bloxham & Gubbins 1987; Kohler & Stevenson 1990; Bloxham & Jackson 1990), but the thermal-wind equations used were geostrophic and did not incorporate the effects of magnetic field. The main purpose of this paper is to develop the theory of boundary-forced thermal winds in rotating stratified hydromagnetic flow and to show that the magnetic field has a major effect of the structure and magnitude of such flow.

There is an extensive literature on linearized solutions for boundary-driven flows in rotating fluids, often in cylindrical or annular geometries or making use of the von Kármán similarity form for flow between rotating disks. For example, steady mechanical forcing by small differential rotation of the upper and lower boundaries has been studied for stratified, non-magnetic flow (Barcilon & Pedlosky 1967*a*, *b*), homogeneous, hydromagnetic flow (Vempaty & Loper 1975) and stratified, hydromagnetic flow (Loper 1975, 1976*a*), while the unsteady spin-up problem has been studied for homogeneous, non-magnetic flow (Greenspan & Howard 1963), homogeneous hydromagnetic flow (Benton & Loper 1969; Loper & Benton 1970), and stratified hydromagnetic flow (Loper 1976*b*, *c*). Interest has focused on the mechanisms by which the boundaries control the interior flow and on the suppression of columnar motion by stratification leading to laminated flow. Thermal forcing has sometimes been considered through the action of centrifugal buoyancy on the mismatch between paraboloidal potential surfaces and horizontal boundaries (e.g. Barcilon & Pedlosky 1967*a*, *c*; Loper 1975), which has obvious applications to laboratory experiments in rotating tanks but is not relevant to the core where the leading-order ellipsoidal boundary with the mantle is an isopotential surface. To our knowledge, stratified hydromagnetic flow driven solely by applied lateral variation in the thermal boundary conditions has not been considered previously.

Mathematically, this problem is linked to the Rayleigh–Bénard problem (Chandrasekhar 1981) and the same differential system is to be solved, the difference being that here the boundary conditions are inhomogeneous and the (stable) stratification prescribed, whereas the classical linear Rayleigh–Bénard problem has homogeneous boundary conditions and the (unstable) stratification appears as an eigenvalue. More recently, large-scale numerical simulations have been able to examine the effects of inhomogeneous boundary conditions on the Rayleigh–Bernard problem in a spherical annulus in both rotating magnetoconvection and numerical dynamos (e.g. Olson & Glatzmeier 1996; Sarson, Jones & Longbottom 1997; Gibbons & Gubbins 2000; Bloxham 2000; Olson & Christensen 2002). Physically, of course, stable stratification has a major effect on the structure of the flow and the present analytic solutions are thus complementary to the numerical investigations for convecting systems. We note that the interactions of stable stratification, rotation and magnetic field allow a variety of free oscillations and wave modes (e.g. Hide 1966, 1969; Braginsky 1967, 1984, 1993), but our interest here is in the flow forced by imposed steady inhomogeneous thermal boundary conditions.

We begin with the problem definition in § 2. The non-magnetic problem is solved in § 3 to contrast with the hydromagnetic solution in § 4. The solution for some other boundary conditions is explored briefly in § 5. The thermally driven hydromagnetic flow involves two vertical lengthscales much shorter than the horizontal wavelength of the forcing and one which is much longer. In § 6 we sketch the great variety of vertical and horizontal lengthscales that could arise in linear motions in a stratified rotating hydromagnetic flow depending on the relative strengths of viscosity, rotation, stratification and magnetic field. This analysis extends Loper's (1976*a*) discussion of boundary-layer scales to include scales of columnar and blocking structures. Finally, we close with a discussion of the application of the analysis to the Earth's core.

2. Problem description

Consider a semi-infinite layer of electrically conducting fluid in $z < 0$, rotating about a vertical axis at angular velocity $\boldsymbol{\Omega} = \Omega \boldsymbol{e}_z$, permeated by a uniform background

vertical magnetic field $\boldsymbol{B}_0 = B\boldsymbol{e}_z$, stably stratified by a background temperature gradient $\mathrm{d}\theta_0/\mathrm{d}z$ and overlain by a rigid, electrically insulating boundary. We are interested in the flow $\boldsymbol{u}$ that is forced by steady lateral variations in the thermal boundary condition imposed at $z = 0$.

The Boussinesq equations governing linearized magnetohydrodynamic motion about this background state (Chandrasekhar 1981, p. 197) are

$$(\partial_t - \nu\nabla^2)\boldsymbol{u} + 2\boldsymbol{\Omega} \wedge \boldsymbol{u} = -\rho_0^{-1}\nabla P + g\alpha\theta\boldsymbol{e}_z + (\rho_0\mu_m)^{-1}(\boldsymbol{B_0}\cdot\nabla)\boldsymbol{b}, \tag{2.1}$$

$$(\partial_t - \eta\nabla^2)\boldsymbol{b} = (\boldsymbol{B_0}\cdot\nabla)\boldsymbol{u}, \tag{2.2}$$

$$\nabla\cdot\boldsymbol{u} = 0, \qquad \nabla\cdot\boldsymbol{b} = 0, \tag{2.3}$$

$$(\partial_t - \kappa\nabla^2)\theta + (\mathrm{d}\theta_0/\mathrm{d}z)w = 0, \tag{2.4}$$

where $\boldsymbol{b}$ and θ are the perturbations to the background field and temperature, $w = \boldsymbol{u}\cdot\boldsymbol{e}_z$ is the vertical velocity and $P = p + \rho_0 gz + \frac{1}{2}(\rho_0|\boldsymbol{\Omega}|^2 + |\boldsymbol{B}|^2/\mu_m)$ is the modified pressure; ρ_0 is the Boussinesq reference density, ν the kinematic viscosity, η the magnetic diffusivity, μ_m the magnetic permeability, κ the thermal diffusivity and α the thermal expansivity of the fluid. In making the Boussinesq approximation, we are assuming either that the effects of compressibility are negligible or that they can be absorbed by definition of a suitable potential temperature. We also assume that gravity dominates centrifugal effects so that the buoyancy term in (2.1) acts vertically.

We introduce the vertical components of vorticity $\zeta = (\nabla\wedge\boldsymbol{u})_z$ and of induced electric current $j = \mu_m^{-1}(\nabla\wedge\boldsymbol{b})_z$. Then successive curling of the momentum and induction equations (2.1) and (2.2), together with use of (2.3), yields the system of scalar equations (Chandrasekhar 1981, p. 199)

$$(\partial_t - \nu\nabla^2)\nabla^2 w + 2\Omega\partial_z\zeta = g\alpha\left(\nabla^2 - \partial_z^2\right)\theta + (B_0/\rho_0\mu_m)\partial_z\nabla^2 b_z, \tag{2.5}$$

$$(\partial_t - \nu\nabla^2)\zeta - 2\Omega\partial_z w = (B_0/\rho_0)\partial_z j, \tag{2.6}$$

$$(\partial_t - \eta\nabla^2)b_z = B_0\partial_z w, \tag{2.7}$$

$$\mu_m(\partial_t - \eta\nabla^2)j = B_0\partial_z\zeta, \tag{2.8}$$

to be solved with (2.4).

We restrict our attention to steady motion ($\partial_t = 0$), leaving the possible temporal instability of finite-amplitude motions for future investigation. It is then possible to eliminate b_z between (2.5) and (2.7) without increasing the order of the system. We non-dimensionalize with respect to a lengthscale L, timescale T, velocity scale L/T, temperature scale $L/(g\alpha T^2)$ and magnetic-field scale $L^2 B_0/(\eta T)$ to obtain

$$-E\nabla^2\nabla^2 w + C\partial_z\zeta = \left(\nabla^2 - \partial_z^2\right)\theta - \Lambda\partial_z^2 w, \tag{2.9}$$

$$-E\nabla^2\zeta - C\partial_z w = \Lambda\partial_z j, \tag{2.10}$$

$$-\nabla^2 j = \partial_z\zeta, \tag{2.11}$$

$$-E\nabla^2\theta + Sw = 0, \tag{2.12}$$

where

$$C = 2\Omega T, \qquad E = \frac{\nu T}{L^2}, \qquad \Lambda = \frac{B_0^2 T}{\rho_0\mu_m\eta}, \qquad S = g\alpha T^2\frac{\mathrm{d}\theta_0}{\mathrm{d}z}\frac{\nu}{\kappa} \tag{2.13}$$

are dimensionless measures of the importance of rotation, viscosity, magnetic field and stratification. It should be noted that L and T can be arbitrary scales, though it is sensible to choose L to be characteristic of the lateral scale of the boundary inhomogeneity and to choose T so that one of C, E, Λ or S is set equal to 1. Indeed, for the rotation-dominated flows of §§ 3–5, we choose $T=(2\Omega)^{-1}$ so that $C=1$, and E and Λ become the Ekman and Elsasser numbers. (In the Rayleigh-Bénard problem one would choose $T=L^2/\nu$, with L the height of a finite layer, so that $E=1$ and $-S$ is the Rayleigh number.) In § 6 we will revert to T being unspecified in order to allow consideration of non-rotating flow as the limit $C\to 0$.

Finally, we note that, since the problem is linear and laterally unbounded, it is sufficient to solve for a single horizontal wavenumber k and obtain the general solution by Fourier superposition. Thus we set $\{w,\zeta,j,\theta\}=\{W(z),Z(z),J(z),\Theta(z)\}\exp(\mathrm{i}kx)$ to obtain the tenth-order ordinary differential system

$$E(\mathrm{D}^2-k^2)^2W=\mathrm{D}Z+\Lambda\mathrm{D}^2W+k^2\Theta, \tag{2.14}$$

$$E(\mathrm{D}^2-k^2)Z=-\mathrm{D}W-\Lambda\mathrm{D}J, \tag{2.15}$$

$$(\mathrm{D}^2-k^2)J=-\mathrm{D}Z, \tag{2.16}$$

$$E(\mathrm{D}^2-k^2)\Theta=SW, \tag{2.17}$$

where D denotes $\mathrm{d}/\mathrm{d}z$. The horizontal velocity components can be recovered from $Z=\mathrm{i}kV$ and $DW=-\mathrm{i}kU$. No-slip insulating boundary conditions $W=\mathrm{D}W=Z=J=0$ apply at $z=0$, together with decay as $z\to-\infty$. The flow is driven by the thermal boundary condition $\Theta(0)=1$.

Solution of this differential system is, of course, mathematically straightforward. In the geophysically relevant limit $E\to 0$, the equations become singular and boundary layers can be expected. The point of physical interest is that the magnetic field causes a major change to the structure of the flow, in particular reducing the magnitude of the thermal wind from $O(1)$ to $O(E^{1/4})$. This change in structure is the focus of the following sections.

3. Non-magnetic flow

We begin by considering (2.14)–(2.17) with $\Lambda=0$, where J and (2.16) can be ignored and the order of the system reduces to eight. The solution can be deduced using the method of Barcilon & Pedlosky (1967*a*), though we present an alternative method here for better comparison with § 4. Note first that the equations can be combined to give

$$(\mathrm{D}^2-k^2)[E^2(\mathrm{D}^2-k^2)^3+\mathrm{D}^2-Sk^2]W=0. \tag{3.1}$$

It follows that for $E\ll 1$ there is a boundary layer with the Ekman scaling $z\sim E^{1/2}$ outside of which the solution is a linear combination of $\exp(kz)$ and $\exp(Kz)$, where $K=S^{1/2}k$.

3.1. *Ekman boundary layer*

With scalings $\mathrm{D}\sim E^{-1/2}$, $W\sim E$, $Z\sim E^{1/2}$, $\Theta\sim 1$, the leading-order equations are

$$E\mathrm{D}^4W=\mathrm{D}Z+k^2\Theta, \tag{3.2}$$

$$E\mathrm{D}^2Z=-\mathrm{D}W, \tag{3.3}$$

$$E\mathrm{D}^2\Theta=0. \tag{3.4}$$

The general solution with no exponential growth is

$$\begin{pmatrix} W/E \\ Z/E^{1/2} \\ \Theta \end{pmatrix} = \frac{c_+}{m_+}\begin{pmatrix} -\mathrm{i} \\ m_+ \\ 0 \end{pmatrix} \mathrm{e}^{(1+\mathrm{i})\zeta} + \frac{c_-}{m_-}\begin{pmatrix} \mathrm{i} \\ m_- \\ 0 \end{pmatrix} \mathrm{e}^{(1-\mathrm{i})\zeta} + \begin{pmatrix} W_0 + k^2\Theta_1\zeta \\ Z_0 - 2^{1/2}k^2\left(\Theta_0\zeta + \frac{1}{2}\Theta_1\zeta^2\right) \\ \Theta_0 + \Theta_1\zeta \end{pmatrix} \quad (3.5)$$

where $2^{1/2}m_\pm = 1 \pm \mathrm{i}$ and $\zeta = z/(2E)^{1/2}$. In order to match Θ outwards to a more slowly varying solution, Θ_1 must be $O(E^{1/2})$. By use of the boundary conditions $Z = W = \mathrm{D}W = 0$ and $\Theta = 1$ at $z = 0$, we get

$$\Theta_0 = 1, \qquad c_+ = c_- = -\frac{Z_0}{2}, \qquad W_0 = -2^{1/2}Z_0. \quad (3.6)$$

Hence,

$$\begin{pmatrix} W/E \\ Z/E^{1/2} \\ \Theta \end{pmatrix} = \begin{pmatrix} -2^{1/2}Z_0(1 - \cos\zeta\,\mathrm{e}^{\zeta} + \sin\zeta\,\mathrm{e}^{\zeta}) \\ Z_0(1 - \cos\zeta\,\mathrm{e}^{\zeta}) - 2^{1/2}k^2\zeta \\ 1 \end{pmatrix}. \quad (3.7)$$

This solution is the superposition of a weak Ekman layer and the edge of a thermal wind. The weakness of the Ekman layer (by a factor $E^{1/2}$) anticipates the matching to the thermal wind in the bulk flow.

3.2. *Geostrophic thermal wind*

Outside the boundary layer, the scaling $\mathrm{D} \sim 1$ suggests $W \sim E$, $Z \sim 1$ and $\Theta \sim 1$, so that the leading-order equations are

$$0 = \mathrm{D}Z + k^2\Theta, \quad (3.8)$$

$$E(\mathrm{D}^2 - k^2)Z = -\mathrm{D}W, \quad (3.9)$$

$$E(\mathrm{D}^2 - k^2)\Theta = SW. \quad (3.10)$$

The scaling of W precludes a stronger Ekman layer. The general solution with decay as $z \to -\infty$ is

$$\begin{pmatrix} W/E \\ Z \\ \Theta \end{pmatrix} = c_1\begin{pmatrix} 0 \\ k \\ -1 \end{pmatrix} \mathrm{e}^{kz} + c_2\begin{pmatrix} K^2 - k^2 \\ -K \\ S \end{pmatrix} \mathrm{e}^{Kz}. \quad (3.11)$$

Matching Z inwards at $O(1)$ to (3.7) gives $c_1 = S^{1/2}c_2$, while matching Θ shows that $c_1 = 1/(S^{1/2} - 1)$. (The case $S = 1$ is degenerate but not singular.) These values of c_1 and c_2 also give the correct matching $\mathrm{D}Z \sim -k^2$ and give $W_0 = k^2(S-1)/(S - S^{1/2})$.

This solution shows some similarity with the analysis (Barcilon & Pedlosky 1967*a*) of stratified rotating flow with $S \gg E^{1/2}$ driven mechanically by a super-rotating boundary. Both solutions show that the interior flow is a geostrophic thermal wind formed by a superposition of a baroclinic and barotropic component. The thermal perturbation extends to an $O(1)$ depth by diffusion and Ekman pumping is suppressed from $O(E^{1/2})$ to $O(E)$ by a linear decrease of the strength of the geostrophic circulation to zero at the boundary. On the other hand, Barcilon & Pedlosky (1967*b*) found that the flow structure changes for $S \ll E^{1/2}$ as the thermal perturbation becomes controlled instead by Ekman pumping. It is interesting to note that this transition is determined by the boundary conditions and is not obvious from the scales inherent in the differential operator. By contrast, no such transition occurs

at $S = O(E^{1/2})$ in the thermally forced flow, and the solution given above holds down to $S = O(E^2)$ at which stage the viscous term needs to be reintroduced in (3.8) since $W \sim E/S^{1/2}$ has become $O(1)$. This transition is inherent in the differential operator (see § 6), as is a different transition that occurs in both the thermally and mechanically forced flows at very strong stratifications; when $S \gg E^{-1}$ the $O(S^{-1/2})$ depth of the baroclinic flow merges with the $O(E^{1/2})$ Ekman layer to form a single $O[(E^2/S)^{1/6}]$ structure.

4. Hydromagnetic flow

Equations (2.14)–(2.17) can be written $\mathscr{L}W = 0$, where $\mathscr{L}$ is the tenth-order operator (Chandrasekhar 1981, p. 200)

$$\mathscr{L} = (\mathrm{D}^2 - k^2)\mathscr{M}^2 + (\mathrm{D}^2 - k^2)^2\mathrm{D}^2 - (Sk^2/E)\mathscr{M} \quad \text{and} \quad \mathscr{M} = E(\mathrm{D}^2 - k^2)^2 - \Lambda\mathrm{D}^2.$$

This operator has three distinguished scalings, $\mathrm{D} \sim E^{-1/2}$, $\mathrm{D} \sim E^{-1/4}$ and $\mathrm{D} \sim E^{1/2}$, corresponding to

$$\mathscr{L} \sim \mathrm{D}^6[(E\mathrm{D}^2 - \Lambda)^2 + 1],$$
$$\mathscr{L} \sim \mathrm{D}^2[\mathrm{D}^4(\Lambda^2 + 1) + Sk^2\Lambda/E],$$
$$\mathscr{L} \sim -(Sk^2/E)(Ek^4 - \Lambda\mathrm{D}^2),$$

respectively. The hydromagnetic problem thus requires matching across a three-layered structure, as described below.

4.1. *Ekman–Hartmann boundary layer*

With scalings $\mathrm{D} \sim E^{-1/2}$, $W \sim E^{3/4}$, $Z \sim E^{1/4}$, $J \sim E^{3/4}$, $\Theta \sim 1$, (2.14)–(2.17) become

$$E\mathrm{D}^4 W = \mathrm{D}Z + \Lambda\mathrm{D}^2 W, \tag{4.1}$$
$$E\mathrm{D}^2 Z = -\mathrm{D}W - \Lambda\mathrm{D}J, \tag{4.2}$$
$$\mathrm{D}^2 J = -\mathrm{D}Z, \tag{4.3}$$
$$E\mathrm{D}^2\Theta = 0. \tag{4.4}$$

The relative scalings of W, Z and J are forced by the balances in (4.1)–(4.3), but the absolute values are a factor $E^{1/4}$ weaker than the usual Ekman–Hartmann scalings (Gilman & Benton 1968; Benton & Loper 1969), anticipating the matching to the thermal wind in § 4.2.

The general solution of (4.1)–(4.4) with no exponential growth is

$$\begin{pmatrix} W/E^{3/4} \\ Z/E^{1/4} \\ J/E^{3/4} \\ \Theta \end{pmatrix} = \frac{c_+}{m_+}\begin{pmatrix} -\mathrm{i} \\ m_+ \\ -1 \\ 0 \end{pmatrix} \mathrm{e}^{(\beta + \mathrm{i}\gamma)\zeta} + \frac{c_-}{m_-}\begin{pmatrix} +\mathrm{i} \\ m_- \\ -1 \\ 0 \end{pmatrix} \mathrm{e}^{(\beta - \mathrm{i}\gamma)\zeta} + \begin{pmatrix} W_0 - \Lambda J_1\zeta \\ Z_0 \\ J_0 + J_1\zeta \\ \Theta_0 + \Theta_1\zeta \end{pmatrix} \tag{4.5}$$

where

$$\beta^2 = (\Lambda^2 + 1)^{1/2} + \Lambda, \qquad \gamma^2 = (\Lambda^2 + 1)^{1/2} - \Lambda, \tag{4.6}$$

$2^{1/2}m_\pm = \beta \pm \mathrm{i}\gamma$ and $\zeta = z/(2E)^{1/2}$. In order to match outwards to a more slowly varying thermal-wind layer, both J_1 and Θ_1 must be $O(E^{1/4})$. By use of the boundary conditions at $z = 0$, we obtain

$$\Theta_0 = 1, \qquad c_+ = c_- = -\frac{Z_0}{2}, \qquad J_0 = -\frac{2^{1/2}\beta Z_0}{\beta^2 + \gamma^2}, \qquad W_0 = -\frac{2^{1/2}\gamma Z_0}{\beta^2 + \gamma^2}. \tag{4.7}$$

Hence,

$$\begin{pmatrix} W/E^{3/4} \\ Z/E^{1/4} \\ J/E^{3/4} \\ \Theta \end{pmatrix} = \begin{pmatrix} W_0[1-\cos(\gamma\zeta)\mathrm{e}^{\beta\zeta}+(\beta/\gamma)\sin(\gamma\zeta)\mathrm{e}^{\beta\zeta}] \\ Z_0[1-\cos(\gamma\zeta)\mathrm{e}^{\beta\zeta}] \\ J_0[1-\cos(\gamma\zeta)\mathrm{e}^{\beta\zeta}-(\gamma/\beta)\sin(\gamma\zeta)\mathrm{e}^{\beta\zeta}] \\ 1 \end{pmatrix} \tag{4.8}$$

where J_0 and W_0 are given by the usual Ekman–Hartmann compatibility conditions (4.7*c*, *d*) in terms of Z_0.

4.2. *Magnetostrophic thermal wind*

Outside the boundary layer, the scaling $\mathrm{D} \sim E^{-1/4}$ suggests $W \sim E^{1/2}$, $Z \sim E^{1/4}$, $J \sim E^{1/2}$ and $\Theta \sim 1$, so that the leading-order equations become

$$0 = \mathrm{D}Z + \Lambda \mathrm{D}^2 W + k^2\Theta, \tag{4.9}$$

$$0 = -\mathrm{D}W - \Lambda \mathrm{D}J, \tag{4.10}$$

$$\mathrm{D}^2 J = -\mathrm{D}Z, \tag{4.11}$$

$$E\mathrm{D}^2\Theta = SW, \tag{4.12}$$

with corrections of relative size $O(E^{1/2})$. The scaling of W precludes a stronger Ekman–Hartmann layer.

The general non-growing solution is

$$\begin{pmatrix} W/E^{1/2} \\ Z/E^{1/4} \\ J/E^{1/2} \\ \Theta \end{pmatrix} = d_+ \begin{pmatrix} \Lambda k^2 \\ (1+\mathrm{i})\delta k^2 \\ -k^2 \\ -2\mathrm{i}\delta^2(1+\Lambda^2) \end{pmatrix} \mathrm{e}^{(1+\mathrm{i})\tilde{\zeta}} + d_- \begin{pmatrix} \Lambda k^2 \\ (1-\mathrm{i})\delta k^2 \\ -k^2 \\ 2\mathrm{i}\delta^2(1+\Lambda^2) \end{pmatrix} \mathrm{e}^{(1-\mathrm{i})\tilde{\zeta}} + \begin{pmatrix} 0 \\ \tilde{Z} \\ \tilde{J} \\ 0 \end{pmatrix} \tag{4.13}$$

where $\delta^4 = k^2 S\Lambda/4(1+\Lambda^2)$ and $\tilde{\zeta} = \delta z/E^{1/4}$. Matching W inwards at $O(E^{1/2})$ to (4.8) shows that $d_+ + d_- = O(E^{1/4})$. Thus

$$\begin{pmatrix} W/E^{1/2} \\ Z/E^{1/4} \\ J/E^{1/2} \\ \Theta \end{pmatrix} = \Delta \begin{pmatrix} \Lambda k^2 \sin\tilde{\zeta} \\ \delta k^2(\sin\tilde{\zeta}+\cos\tilde{\zeta}) \\ -k^2\sin\tilde{\zeta} \\ -2\delta^2(1+\Lambda^2)\cos\tilde{\zeta} \end{pmatrix} \mathrm{e}^{\tilde{\zeta}} + \Sigma \begin{pmatrix} \Lambda k^2 \cos\tilde{\zeta} \\ \delta k^2(\cos\tilde{\zeta}-\sin\tilde{\zeta}) \\ -k^2\cos\tilde{\zeta} \\ 2\delta^2(1+\Lambda^2)\sin\tilde{\zeta} \end{pmatrix} \mathrm{e}^{\tilde{\zeta}} + \begin{pmatrix} 0 \\ \tilde{Z} \\ \tilde{J} \\ 0 \end{pmatrix} \tag{4.14}$$

where $\Sigma = O(E^{1/4})$. Matching Θ and Z inwards to (4.8) gives

$$\Delta = -[k^2 S\Lambda(1+\Lambda^2)]^{-1/2}, \qquad \tilde{Z} = Z_0 - \Delta\delta k^2. \tag{4.15}$$

Matching W and J inwards at $O(E^{3/4})$ gives

$$\Sigma = \frac{E^{1/4}W_0}{\Lambda k^2}, \qquad \tilde{J} = E^{1/4}(J_0 + W_0\Lambda^{-1}). \tag{4.16}$$

That $\tilde{J} = O(E^{1/4})$ will prove to be consistent with the scale of J in the outer layer.

4.3. *Outer diffusive layer – remnant disturbance*

The scaling $\mathrm{D} \sim E^{1/2}$ suggests $W \sim E^{7/4}$, $Z \sim E^{1/4}$, $J \sim E^{3/4}$ and $\Theta \sim E^{3/4}$, so that the leading-order equations become

$$0 = \mathrm{D}Z + k^2\Theta, \tag{4.17}$$

$$-Ek^2 Z = -\Lambda \mathrm{D}J, \tag{4.18}$$

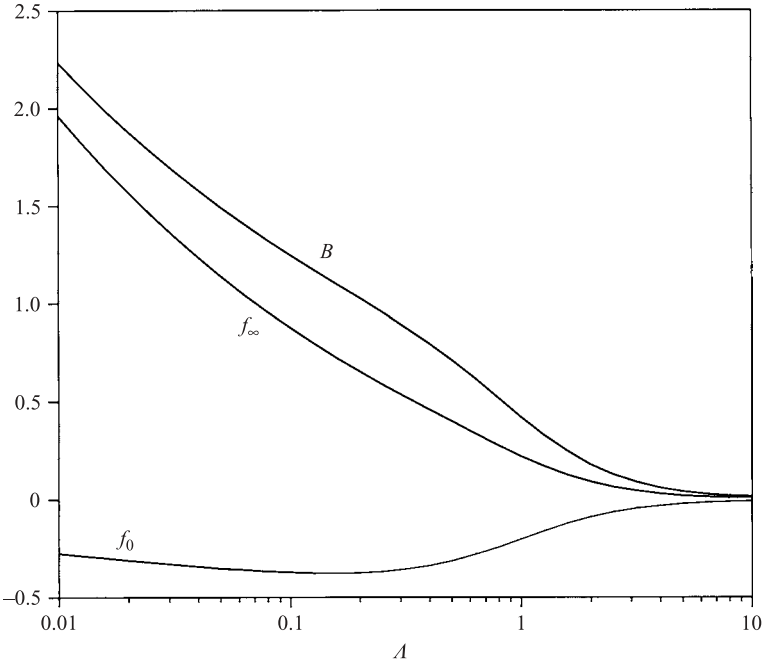

FIGURE 1. The functions $f_0(\Lambda) = -B/(1+A)$ and $f_\infty(\Lambda) = AB/(1+A)$, defined by (4.24) and (4.25), describe the strength of the thermal wind for the boundary conditions of § 4. For the free-slip boundary conditions of § 5.1 they are replaced by $f_\infty = 0$ and $f_0 = -B$; with a rigid bottom in § 5.2 they are replaced by $f_\infty = B/2$ and $f_0 = -B/2$.

$$-k^2 J = -\mathrm{D}Z, \tag{4.19}$$

$$-Ek^2\Theta = SW. \tag{4.20}$$

The general decaying solution is

$$\begin{pmatrix} W/E^{7/4} \\ Z/E^{1/4} \\ J/E^{3/4} \\ \Theta/E^{3/4} \end{pmatrix} = \frac{Z_\infty}{\Lambda^{1/2}} \begin{pmatrix} k^2/S \\ \Lambda^{1/2} \\ 1 \\ -1 \end{pmatrix} \exp\left[(E/\Lambda)^{1/2}k^2 z)\right]. \tag{4.21}$$

Matching Z and J inwards to (4.14) shows that $\tilde{Z} = Z_\infty$ and $\tilde{J} = Z_\infty E^{1/4}/\Lambda^{1/2}$. Comparison with (4.16*b*) and (4.15*b*) gives

$$Z_\infty = J_0\Lambda^{1/2} + W_0\Lambda^{-1/2} = -A(\Lambda)Z_0, \tag{4.22}$$

$$Z_\infty = Z_0 + B(\Lambda)k^{3/2}S^{-1/4}, \tag{4.23}$$

where

$$A(\Lambda) = \frac{\beta\Lambda^{1/2} + \gamma\Lambda^{-1/2}}{[2(1+\Lambda^2)]^{1/2}}, \qquad B(\Lambda) = \frac{1}{[4\Lambda(1+\Lambda^2)^3]^{1/4}}, \tag{4.24}$$

and β and γ are given by (4.6). Thus

$$Z_0 = k^{3/2}S^{-1/4} f_0(\Lambda), \qquad Z_\infty = k^{3/2}S^{-1/4} f_\infty(\Lambda), \tag{4.25}$$

where $f_0(\Lambda) = -B/(1+A)$ and $f_\infty(\Lambda) = AB/(1+A)$. These functions are shown in figure 1.

The structure of the forced thermal wind in the presence of magnetic field is thus very different from the non-magnetic flow of § 3. Only the inner $E^{1/2}$ viscous boundary layer is similar, with the magnetic field simply producing a modification from Ekman to Ekman–Hartmann structure. However, the thermal wind is confined by magnetic effects to a thin layer of thickness $E^{1/4}$ and the amplitude of the thermal wind is correspondingly reduced from $O(1)$ to $O(E^{1/4})$ for unit thermal forcing. This reduction is an important effect when making predictions of flow in the Earth's core. In hydromagnetic flow, coupling between the vertical current and vorticity also allows the thermal wind to drive columnar motion to a large depth $O(E^{-1/2})$.

5. Other boundary conditions

We have found the hydromagnetic flow driven by lateral variation in thermal boundary conditions for the simplest case of a half-space overlain by a rigid insulating boundary. Here we sketch a few ways that the solution can be adapted to other boundary conditions.

5.1. *A free-slip top boundary*

Suppose we now change the top boundary conditions to $W = \mathrm{D}^2 W = \mathrm{D}Z = J = 0$ corresponding to impenetrable, free-slip, insulating conditions. The solution for the thermal wind is still (4.14)–(4.16). Because the Ekman–Hartmann layer now only has to adapt to free-slip conditions, it is a factor $E^{1/4}$ weaker, and hence J_0 and W_0 are $O(E^{1/4})$, and $\tilde{J}$ and Σ are $O(E^{1/2})$. By matching outwards, $\tilde{Z} = Z_\infty$ is $O(E^{1/4})$ and hence $Z_0 = \Delta\delta k^2$ or $f_0 = -B$. In this case, the leading-order thermal wind in the middle layer is just the term with coefficient Δ in (4.14) and can be found directly from the thermal forcing. The inner and outer solutions are higher-order effects.

5.2. *A rigid insulating bottom boundary*

Suppose instead we change the boundary conditions from decay as $z \to -\infty$ to $W = \mathrm{D}W = Z = J = \Theta = 0$ at $z = -H$ corresponding to a rigid, electrically insulating, isothermal lower boundary. Provided $H \ll E^{-1/2}$, the leading-order behaviour outside the $E^{1/2}$ and $E^{1/4}$ boundary layers is given by $\mathrm{D}Z = \mathrm{D}J = 0$ instead of (4.18) and (4.19). Thus $Z = E^{1/4} Z_\infty$ and $J = E^{3/4} J_\infty$, where Z_∞ and J_∞ must both be found by matching.

Near $z = -H$ there is an Ekman–Hartmann layer given by (Gilman & Benton 1968; Benton & Loper 1969)

$$\begin{pmatrix} W/E^{3/4} \\ Z/E^{1/4} \\ J/E^{3/4} \\ \Theta \end{pmatrix} = \begin{pmatrix} W_1[1 - \cos(\gamma\eta)\mathrm{e}^{-\beta\eta} - (\beta/\gamma)\sin(\gamma\eta)\mathrm{e}^{-\beta\eta}] \\ Z_1[1 - \cos(\gamma\eta)\mathrm{e}^{-\beta\eta}] \\ J_1[1 - \cos(\gamma\eta)\mathrm{e}^{-\beta\eta} + (\gamma/\beta)\sin(\gamma\eta)\mathrm{e}^{-\beta\eta}] \\ 0 \end{pmatrix} \tag{5.1}$$

where $\eta = (z + H)/(2E)^{1/2}$ and

$$J_1 = \frac{2^{1/2}\beta Z_1}{\beta^2 + \gamma^2}, \qquad W_1 = \frac{2^{1/2}\gamma Z_1}{\beta^2 + \gamma^2}. \tag{5.2}$$

The Ekman–Hartmann layer is nested within an $E^{1/4}$ layer analogous to (4.14), with constants Δ_1, Σ_1, $\tilde{Z}_1$ and $\tilde{J}_1$. In this case matching Θ and Z to (5.1) gives $\Delta_1 = 0$ and $\tilde{Z}_1 = Z_1$, so that there is no thermal wind at the bottom boundary at leading order. Matching W and J to (5.1) gives $\tilde{J}_1 = E^{1/4}(J_1 + W_1 \Lambda^{-1})$, showing that the $E^{1/4}$ layer is non-trivial even though there is no leading-order thermal wind. Finally, matching

the $E^{1/4}$ layer to the bulk solution gives $\tilde{J}_1 = E^{1/4} J_\infty$ and $\tilde{Z}_1 = Z_\infty$. Thus (4.23) is replaced by $Z_\infty = -Z_0$ and combination with (4.23) gives $f_\infty = B/2$ and $f_0 = -B/2$ (figure 1).

While the change to the boundary conditions, both here and in § 5.1, affects the numerical values of the various constants, it does not affect the scalings of the thermal wind with E, k and S.

5.3. *Heat-flux variations*

The solution for the boundary condition $\mathrm{D}\Theta = 1$, corresponding to imposed heat flux variations rather than imposed temperature variations, can simply be obtained by rescaling the solutions given above. For non-magnetic flow we rescale (3.11) by $(S^{1/2}-1)/(S-1)$, whereas for hydromagnetic flow we rescale (4.14) by $E^{1/4}/\delta$ reducing the strength of the thermal wind further to $O(E^{1/2} k S^{-1/2})$.

6. General exploration of the scales in linear flows

In § 4 we constructed the flow by noting that the tenth-order operator $\mathscr{L}$ has three distinguished scalings for the vertical derivative D as $E \to 0$, with Λ and S both $O(1)$. The dependence of the depth of the magnetostrophic thermal wind (4.14) on both Λ and S raises the question of whether the solution structure changes as these parameters become asymptotically large or small. More generally, one can ask what vertical and horizontal scales can be supported by the differential system (2.9)–(2.12) as $E \to 0$ for different scalings of the parameters C, Λ and S with E. (In this section we reintroduce C as an independent parameter to allow consideration of non-rotating flow as the limit $C \to 0$.) This question was partly answered by Loper (1976*a*) who, while considering mechanically driven stratified hydromagnetic flow in a rotating cylinder, identified the possible horizontal and vertical boundary-layer scalings that might arise in such a flow i.e. the scales that are much shorter than the scale of the boundary forcing. Here we also consider scales much longer than the scale of the forcing, such as the columnar motions of § 4.3, the Taylor column associated with motion of a small body through a large volume of fluid, or the phenomenon of blocking in stratified flow.

The method followed is the same as that of Loper (1976*a*), namely to look for self-consistent asymptotic balances between two of the terms labelled [*a*]–[*e*] in the operator

$$\underset{[a]}{\mathscr{L}} \equiv \underset{[a]}{E\nabla^2(E\nabla^4 - \Lambda \mathrm{D}^2)^2} + \underset{[b]}{EC^2\nabla^4\mathrm{D}^2} - \underset{[c]}{S(\nabla^2 - \mathrm{D}^2)(E\nabla^4 - \Lambda\mathrm{D}^2)} = 0 \qquad (6.1)$$

that results from (2.9)–(2.12). As in the previous sections, we look for solutions proportional to $\exp(\mathrm{i}kx + mz)$, where x is a horizontal coordinate, from which the general solution can be obtained by Fourier superposition (k and m are not necessarily real). The operators ∇^2 and D^2 produce $m^2 - k^2$ and m^2 respectively, and the asymptotic roots $m(k)$ and $k(m)$ resulting from different balances in (6.1) are given in table 1, with the regions of validity for these balances summarized in figures 2–4. Table 1 extends tables 2 and 3 of Loper (1976*a*) by giving the long scales as well as the short and by including the $O(1)$ numerical coefficients. Figures 2–4 are consistent with figures 1 and 2 of Loper (1976*a*), but are drawn to show the ten roots $m(k)$ and $k(m)$ for all parameter values.

It should be noted that, by virtue of independence of the arbitrary scales L and T used in the non-dimensionalization, the results only depend on the parameter

Label	Balance	$m^2(k)$	$k^2(m)$
$A1$	a, c	$\pm iC/E$	—
$A2a$	a, b	Λ/E twice	—
$A2b$	d, e	Λ/E once	—
$A4$	a, d	$(Sk^2/E^2)^{1/3}$	E^2m^6/S
$A5$	c, d	Sk^2/C^2	C^2m^2/S
$A6$	b, e	$(-Sk^2/E\Lambda)^{1/2}$	$-E\Lambda m^4/S$
$A7$	c, e	$(-S\Lambda k^2/EC^2)^{1/2}$	$-EC^2m^4/S\Lambda$
$B1$	a, c	$-E^2k^6/C^2$	$(C^2m^2/E^2)^{1/3}$
$B2a$	a, b	Ek^4/Λ twice	$(\Lambda m^2/E)^{1/2}$ twice
$B2b$	d, e	Ek^4/Λ once	$(\Lambda m^2/E)^{1/2}$ once
$B3$	b, c	C^2k^2/Λ^2	Λ^2m^2/C^2
$B4$	a, d	—	$(S/E^2)^{1/2}$
$B5$	c, d	Sk^2/C^2	C^2m^2/S
$B6$	b, e	$-S/E\Lambda$	—
$B7$	c, e	—	$S\Lambda/EC^2$
$C1$	d	k^2 twice	m^2 twice
$C2$	c	k^2 twice	m^2 twice
$C3$	b	k^2 once	m^2 once
$C4$	a	k^2 (5 times)	m^2 (5 times)

TABLE 1. The dimensionless inverse vertical and horizontal scales m and k resulting from different balances in (6.1) for modes proportional to $\exp(ikx + mz)$. The labels are based on Loper (1976*a*) with An used for $|k| \ll |m|$, Bn used for $|m| \ll |k|$ and Cn used for $|m| \sim |k|$. Fractional powers include all the complex roots, and some solutions have the multiplicity shown. The regions of validity are shown in figures 2 and 3.

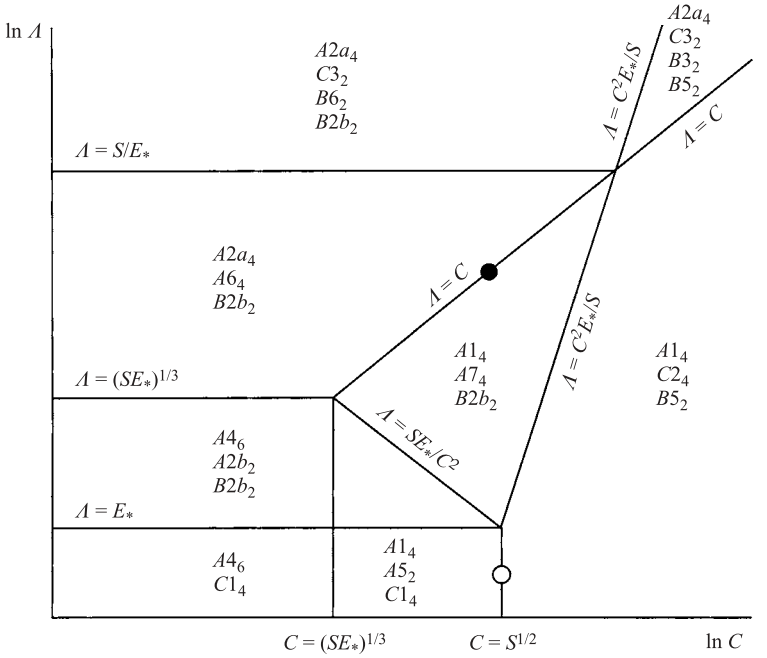

FIGURE 2. Regions of validity for the roots $m(k)$ in table 1 for $S \gg E_*^2$, where $E_* = Ek^2$. The subscripts on the roots show multiplicity, and there are 10 roots in all regions. The analyses of § 3 and § 4 lie at the points marked ○ and ●.

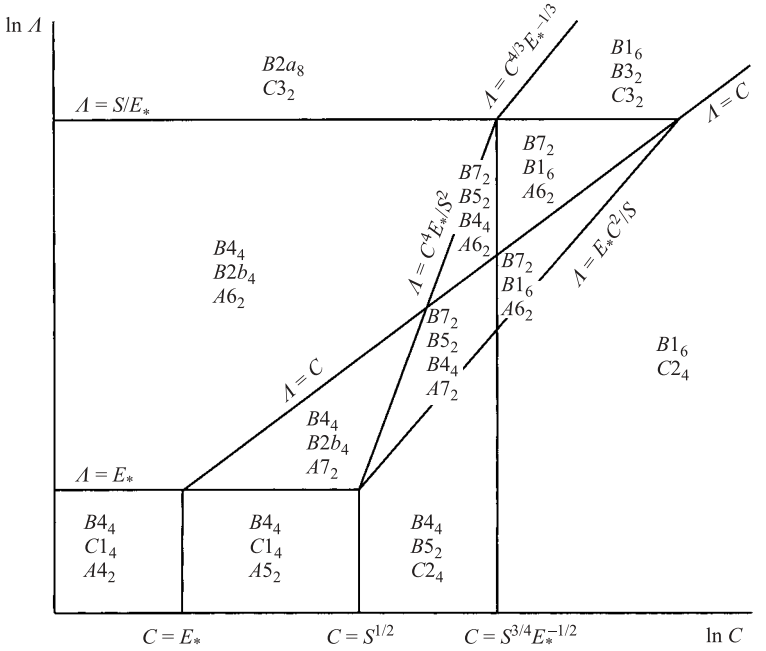

FIGURE 3. Regions of validity for the roots $k(m)$ in table 1 for $S \gg E_*^2$, where $E_* = Em^2$.

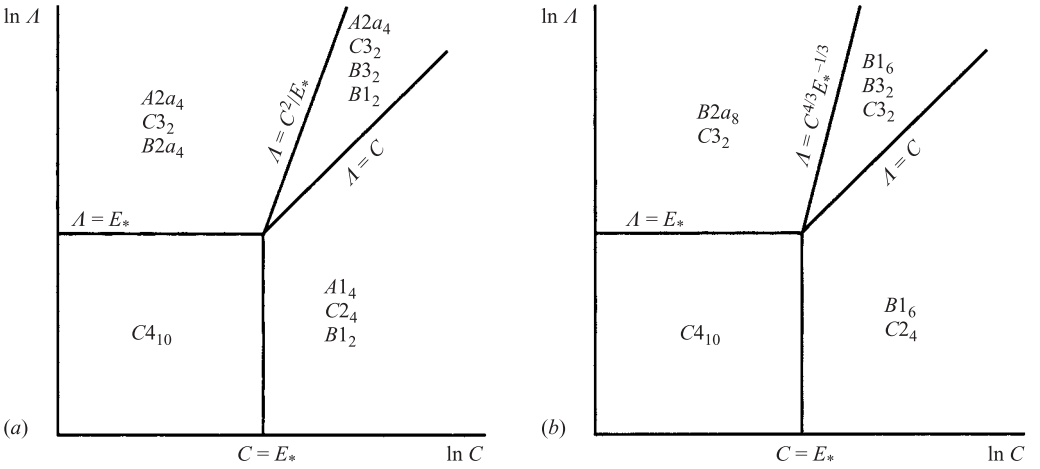

FIGURE 4. Regions of validity for $S \ll E_*^2$: (*a*) $m(k)$; (*b*) $k(m)$.

combinations C/E_*, Λ/E_* and S/E_*^2, where $E_* = Ek^2$ or Em^2 is the Ekman number based on the lengthscale L/k or L/m, respectively. Depending on the problem, it may be sensible to choose T so that one of C, Λ or S is set equal to 1.

Within this larger context, it can be seen that the non-magnetic thermal wind of § 3 with $C = 1$ and $S = O(1)$ is constructed from m-roots $A1$, $A5/B5$ and $C1/C2$, while the hydromagnetic thermal wind of § 4 and § 5 with $C = 1$ and S, $\Lambda = O(1)$ is constructed from $A1/A2a$, $A6/A7$ and $B2b$ (figure 2). (Here X/Y denotes the asymptotic overlap between two regimes X and Y.) As mentioned previously, the non-magnetic thermal wind changes scalings at $S = O(E_*^{-1})$ when the baroclinic flow $A5$ and Ekman layer

$A1$ merge to form a stratified Ekman layer $A4$, and at $S = O(E_*^2)$ when the baroclinic flow $B5$ acquires the viscous columnar structure $B1$. The hydromagnetic thermal wind can change scalings in a variety of ways if S and Λ cease to be $O(1)$, at $\Lambda = O(S/E_*)$, $\Lambda = O(SE_*^{1/3})$, $\Lambda = O(E_*/S)$ or $\Lambda = O(E_*S)$. In the mechanically forced non-magnetic flow in a cylinder analysed by Barcilon & Pedlosky (1967*b*), the merging at $S = O(E^{2/3})$ of the hydrostatic and buoyancy sidewall boundary layers, given by k-roots $B4$ and $B5$, to form a Stewartson $E^{1/3}$ layer, given by $B1$, can also be identified in figure 3.

Not all spatial scalings are inherent in the differential operator $\mathscr{L}$ of (6.1) and can thus be found in table 1 and figures 2–4. For example, the Stewartson $E^{1/4}$ vertical shear layer acquires its scaling in part from the requirement that it accommodate the $E^{1/2}$ flux from Ekman pumping. In a spherical annulus the Stewartson-layer scaling is $E^{2/7}$ (Stewartson 1966) within the tangent cylinder because the Ekman flux is $E^{3/7}$, owing to the inclination of the inner-sphere boundary. The scale of the flux is not built into $\mathscr{L}$ and thus these Stewartson scalings are not found in table 1. Moreover, the change in the scaling of W at $S = O(E^{1/2})$ found by Barcilon & Pedlosky (1967*b*) for mechanically forced non-magnetic flow in a cylinder (and similar changes found by Loper (1976*a*) for the hydromagnetic analogue) is not associated with a change in the vertical structure, but simply in the magnitude of the flow in each layer. Such changes are a function of the boundary conditions and not inherent in $\mathscr{L}$. For example, while the scaling of W changes at $S = O(E_*^{1/2})$ in a mechanically forced finite-depth container, it changes at $S = O(E_*)$ in a mechanically forced half-space and is unchanged down to the $B5$–$B1$ transition at $S = O(E_*^2)$ in a thermally forced half-space. While such changes of scale need to be considered on a case-by-case basis, the scales in table 1 are a general property of the differential operator $\mathscr{L}$.

It is straightforward to generalize the analysis to consider the case where $\boldsymbol{B}_0$ and $\boldsymbol{\Omega}$ are no longer parallel to $\boldsymbol{e}_z$; the result is simply to amend $\mathscr{L}$ in (6.1) by replacing $\Lambda \mathrm{D}^2$ by $\Lambda(\hat{\boldsymbol{B}}_0 \cdot \nabla)^2$ and $C^2\mathrm{D}^2$ by $C^2(\hat{\boldsymbol{\Omega}}_0 \cdot \nabla)^2$, where $\hat{\boldsymbol{B}}_0$ and $\hat{\boldsymbol{\Omega}}$ are unit vectors in the directions of $\boldsymbol{B}_0$ and $\boldsymbol{\Omega}$. Without going into detail, we can say that generically the 'long horizontal' scales $A4$, $A5$, $A6$ and $A7$ in table 1 remain horizontal, the 'long vertical' scales $B1$ and $B5$ become elongated in the $\boldsymbol{\Omega}$-direction, the 'long vertical' scales $B2$, $B3$ and $B6$ become elongated in the $\boldsymbol{B}_0$-directions, and some of the 'short horizontal' and 'vertical' scales similarly become oriented by $\boldsymbol{\Omega}$ or $\boldsymbol{B}_0$ instead of $\boldsymbol{e}_z$. New scalings can arise for linear modes in which $\hat{\boldsymbol{B}}_0 \cdot \nabla$, $\hat{\boldsymbol{\Omega}}_0 \cdot \nabla$ or $\hat{\boldsymbol{e}}_z \cdot \nabla$ is almost zero, particularly in the degenerate cases $\boldsymbol{B}_0 \cdot \boldsymbol{e}_z = 0$, $\boldsymbol{\Omega} \cdot \boldsymbol{e}_z = 0$ and $\boldsymbol{\Omega} \cdot \boldsymbol{B}_0 = 0$.

The results of the present analysis cannot easily be compared with those of Shimizu & Loper (1997) who considered the case $S = 0$ with $\boldsymbol{\Omega}$ perpendicular to $\boldsymbol{B}_0$. When $S = 0$ with $\boldsymbol{\Omega}$ parallel to $\boldsymbol{B}_0$ the possible scales are limited to those in figure 4 (i.e. those in table 1 that are independent of S). These scales are also found among the wake modes and boundary-layer scalings of Shimizu & Loper (1997), together with scalings arising from $\boldsymbol{\Omega} \cdot \boldsymbol{B}_0 = 0$. Clearly, the addition of stratification allows more possibilities.

7. Discussion

We have shown that the presence of a magnetic field has a major effect on the strength and structure of the thermal wind generated by lateral variations in the thermal boundary conditions of a stably stratified electrically conducting fluid. While this accords with a general tendency for magnetic fields to resist deformation by flow, it is worth exploring the mechanism that gives rise to the thermal wind with $E^{1/4}$ scaling.

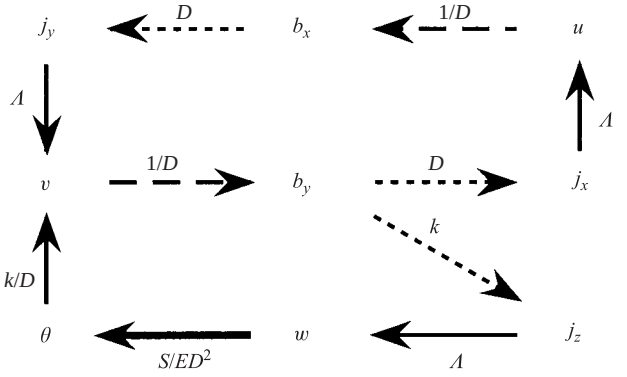

FIGURE 5. The coupling between the variables in the hydromagnetic thermal wind through the vorticity equation (solid arrows), induction equation (dashed), heat equation (bold) and $\mu_m \boldsymbol{j} = \nabla \wedge \boldsymbol{b}$ (dotted). The associated factors give rise to the scaling $D \sim [Sk^2\Lambda/E(1+\Lambda^2)]^{1/4}$.

The ODE system (4.9)–(4.12) can be retraced to the approximate dimensionless forms of the vorticity, induction and heat equations,

$$-2\partial_z \boldsymbol{u} = -ik\theta \boldsymbol{e}_y + \Lambda \partial_z \boldsymbol{j}, \tag{7.1}$$

$$\partial_z^2 \boldsymbol{b} = \partial_z \boldsymbol{u}, \tag{7.2}$$

$$E\partial_z^2 \theta = Sw, \tag{7.3}$$

where the current $\boldsymbol{j}$ is approximated by

$$\boldsymbol{j} = (-\partial_z b_y, \partial_z b_x, ikb_y) \tag{7.4}$$

since $\partial_z b_x \gg \partial_x b_z$. (Note that the horizontal components of $\boldsymbol{u}$, $\boldsymbol{b}$ and $\boldsymbol{j}$ are each a factor $E^{-1/4}$ larger than the corresponding vertical components.) Equation (7.1) states that, with negligible viscosity, distortion of the background vorticity $(\boldsymbol{\Omega} \cdot \nabla)\boldsymbol{u}$ balances the gravitational and Lorentz torques. Equation (7.2) balances vertical diffusion of the perturbation field with distortion of background field $(\boldsymbol{B}_0 \cdot \nabla)\boldsymbol{u}$.

The coupled system of variables is shown schematically in figure 5. For $\Lambda \ll 1$ the lower loop is dominant: horizontal temperature gradients drive a geostrophic thermal wind v; the induced field b_y provides a vertical torque proportional to Λj_z; the resultant upwelling w confines the thermal wind to an $O[(E/Sk^2\Lambda)^{1/4}]$ distance from the boundary. In this regime $v = O[(Ek^2/\Lambda S)^{1/4}]$ for $\theta \sim 1$ and $u \sim \Lambda v \ll v$. For $\Lambda \gg 1$ both loops are important: the induced field b_y not only provides upwelling as before, but also provides a horizontal torque proportional to Λj_x that drives a strong flow u ($\gg v$); further feedback via the induction equation generates a strong field b_x and stronger torque Λj_y; the net effect is that the gravitational torque is almost perfectly counterbalanced by the y-component of the Lorentz torque so that $v = O[(Ek^2/S)^{1/4}\Lambda^{-7/4}]$ and not the $O[(Ek^2\Lambda/S)^{1/4}]$ that might be expected in an $O[(E\Lambda/Sk^2)^{1/4}]$ thick thermal wind. It should be noted that none of this coupling relies upon the Ekman pumping or Hartmann current from the Ekman–Hartmann layer; these turn out to be sufficiently strong to affect the $O(1)$ prefactors of the thermal wind, but not its scaling.

For the Earth's core the main issue is not the scaling with Λ, but the scaling with E. With a typical lengthscale $L = 1000\,\mathrm{km}$, an f-plane approximation $f = 10^{-4}\,\mathrm{s}^{-1}$ to $2\Omega \sin\theta$ and a molecular value $\nu = 10^{-6}\,\mathrm{m}^2\,\mathrm{s}^{-1}$ for the kinematic viscosity of the outer core, we obtain $E = 10^{-14}$. It is sometimes suggested that an eddy viscosity

$\nu = 1\,\mathrm{m^2\,s^{-1}}$ might be more appropriate for turbulent motion in the core, leading to $E = 10^{-8}$. In either case, the $E^{1/4}$ scaling is clearly a significant factor in the estimated size of thermal winds driven by a given spatial variation of the heat flux across the core–mantle boundary. For example, a uniform rate of cooling 20% less than the rate of conduction up the core adiabat would lead to a stratified layer in the outer core about 200 km thick with $S = 0.5$ (Lister & Buffett 1998). The r.m.s. radial field of 0.5 mT with $\rho = 10^4\,\mathrm{kg\,m^{-3}}$ and $\eta = 2\,\mathrm{m^2\,s^{-1}}$ (Stacey 1992) corresponds to $\Lambda = 0.1$. If the magnetic effects are neglected then a mere 5% lateral variation in heat flux would drive a geostrophic thermal wind of magnitude $1\,\mathrm{m\,s^{-1}}$ through the 200 km depth of the stratified layer, which is clearly inconsistent with observed velocities of order $0.3\,\mathrm{mm\,s^{-1}}$. However, if the magnetic effects are included then, with $E = 10^{-14}$ ($E = 10^{-8}$), the thermal wind would be confined to a layer of thickness of order 1 km (35 km) and have a greatly reduced magnitude of order $0.01\,\mathrm{mm\,s^{-1}}$ ($7\,\mathrm{mm\,s^{-1}}$). While there is considerable uncertainty in this calculation about the effective viscosity due to turbulence, it is clear that the magnetic field has a major effect and that the predicted magnitudes of hydromagnetic flow are much easier to reconcile with observations than those of geostrophic flow. Somewhat fortunately, since Λ is small, the direction of hydromagnetic flow for a given pattern of thermal forcing is almost the same as that of the corresponding geostrophic flow, and so previous comments on the similarity between inferred mantle temperatures and core flow patterns (e.g. Bloxham & Gubbins 1987; Kohler & Stevenson 1990; Bloxham & Jackson 1990) may still be significant. Further work will be required to incorporate the variations of f with latitude and B_0 with position into the theory.

I am very grateful to the Research School of Earth Sciences (ANU, Canberra) and the Institut de Physique du Globe (Paris) for hospitality and support in visiting positions during the writing of this manuscript.

REFERENCES

Artyushkov, E. V. 1972 Density differentiation of the Earth's matter and processes at the core-mantle interface. *J. Geophys. Res.* **77**, 6454–6458.

Barcilon, V. & Pedlosky, J. 1967*a* Linear theory of rotating stratified fluid motions. *J. Fluid Mech.* **29**, 1–16.

Barcilon, V. & Pedlosky, J. 1967*b* A unified linear theory of homogeneous and stratified rotating fluids. *J. Fluid Mech.* **29**, 609–621.

Barcilon, V. & Pedlosky, J. 1967*c* On the steady motions produced by a stable stratification in a rapidly rotating fluid. *J. Fluid Mech.* **29**, 673–690.

Benton, E. R. & Loper, D. E. 1969 On the spin-up of an electrically conducting fluid Part 1. The unsteady hydromagnetic Ekman-Hartmann layer problem. *J. Fluid Mech.* **39**, 561–568.

Bloxham, J. 2000 Sensitivity of the geomagnetic axial dipole to thermal core–mantle interactions. *Nature* **405**, 63–65.

Bloxham, J. & Gubbins D. 1987 Thermal core–mantle interactions. *Nature* **325**, 511–513.

Bloxham, J. & Jackson, A. 1990 Lateral temperature variations at the core-mantle boundary deduced from the magnetic field. *Geophys. Res. Lett.* **17**, 1997–2000.

Braginsky, S. I. 1967 Magnetic waves in the Earth's core. *Geomag. Aeron.* **7**, 851–859.

Braginsky, S. I. 1984 Short-period geomagnetic secular variation. *Geophys. Astrophys. Fluid Dyn.* **30**, 1–78.

Braginsky, S. I. 1993 MAC-oscillations of the hidden ocean of the core. *J. Geomag. Geoelectr.* **45**, 1517–1538.

Chandrasekhar, S. 1981 *Hydrodynamic and Hydromagnetic Stability*. Dover.

Fearn, D. R. & Loper, D. E. 1981 Compositional convection and stratification of the Earth's core. *Nature* **289**, 393–394.

Gibbins, S. J. & Gubbins, D. 2000 Convection in the Earth's core driven by lateral variations in the core-mantle boundary heat flux. *Geophys. J. Intl* **142**, 631–642.

Gilman, P. A. & Benton, E. R. 1968 Influence of an axial magnetic field on the steady linear Ekman layer. *Phys. Fluids* **11**, 2397–2401.

Greenspan, H. P. & Howard, L. N. 1963 On a time-dependent motion of a rotating fluid. *J. Fluid Mech.* **17**, 385–404.

Gubbins, D., Thomson, C. J. & Whaler, K. A. 1982 Stable regions in the Earth's liquid core. *Geophys. J. R. Astron. Soc.* **68**, 241–251.

Hide, R. 1966 Free hydromagnetic oscillations of the Earth's core and the theory of the geomagnetic secular variation. *Phil. Trans. R. Soc. Lond.* A **259**, 615–647.

Hide, R. 1969 On hydromagnetic waves in a stratified rotating compressible fluid. *J. Fluid Mech.* **39**, 283–287.

Kohler, M. D. & Stevenson, D. J. 1990 Modelling core-fluid motions and the drift of magnetic field patterns at the CMB by use of topography obtained by seismic inversion. *Geophys. Res. Lett.* **17**, 1473–1476.

Labrosse, S., Poirier, J. P. & Le Mouël, J. L. 1997 On cooling of the Earth's core. *Phys. Earth Planet. Inter.* **99**, 1–17.

Lay, T. & Young, C. J. 1990 The stably stratified outermost core revisited. *Geophys. Res. Lett.* **17**, 2001–2004.

Lister, J. R. & Buffett, B. A. 1998 Stratification of the outer core at the core-mantle boundary. *Phys. Earth Planet. Inter.* **105**, 5–19.

Lloyd, D. & Gubbins, D. 1990 Toroidal fluid motion at the top of Earth's core. *Geophys. J. Intl* **100**, 455–467.

Loper, D. E. 1975 A linear theory of rotating, thermally stratified, hydromagnetic flow. *J. Fluid Mech.* **72**, 1–16.

Loper, D. E. 1976*a* A study of stably stratified fluid in a rotating cylinder. *J. Fluid Mech.* **73**, 529–564.

Loper, D. E. 1976*b* On the spin-up of a stably stratified, electrically conducting fluid. Part I Spin-up controlled by the Hartmann layer. *Geophys. Fluid Dyn.* **7**, 133–156.

Loper, D. E. 1976*c* On the spin-up of a stably stratified, electrically conducting fluid. Part II Spin-up controlled by the MAC layer *Geophys. Fluid Dyn.* **7**, 175–203.

Loper, D. E. & Benton, E. R. 1970 On the spin-up of an electrically conducting fluid Part 2. Hydromagnetic spin-up between infinite flat insulating plates. *J. Fluid Mech.* **43**, 785–799.

Olson, P. & Christensen, U. R. 2002 The time-averaged magnetic field in numerical dyanmos with non-uniform boundary heat flow. *Geophys. J. Intl* **151**, 809–823.

Olson, P. & Glatzmeier, G. A. 1996 Magnetoconvection and thermal coupling of the Earth's core and mantle. *Phil. Trans. R. Soc. Lond.* A **354**, 1413–1424.

Sarson, G. R., Jones, C. A. & Longbottom, A. W. 1997 The influence of boundary region heterogeneities on the geodynamo. *Phys. Earth Planet. Inter.* **101**, 13–32.

Shimizu, H. & Loper, D. E. 1997 Time and length scales of buoyancy driven structures in a rotating hydromagnetic fluid. *Earth Planet. Sci. Lett.* **104**, 307–329.

Stacey, F. D. 1992 *Physics of the Earth*, 3rd edn. Brookfield Press, Brisbane.

Stewartson, K. 1966 On almost rigid rotations. Part 2. *J. Fluid Mech.* **26**, 131–144.

Vempaty, S. & Loper, D. E. 1975 Hydromagnetic boundary layers in a rotating cylindrical container. *Phys. Fluids* **18**, 1678–1686.

Whaler, K. 1980 Does the whole of the Earth's core convect? *Nature*, **287**, 528–530.